# Electrostatic Separation of two Types of Copper Wires from Electric Cable Wastes

Gontran Richard[1, 2], Abdelhady Ragab Salama[1, 3], Karim Medles[1, 4], Cedric Lubat[1, 2], Seddik Touhami[1, 4], Lucian Dascalescu[1]

[1] PPRIME Institute, CNRS - University of Poitiers – ENSMA, IUT, Angoulême, France
[2] CITF, Saint Cybardeaux, France
[3] Shoubra Faculty of Engineering, Benha University, Cairo, Egypt
[4] University of Sidi-Bel-Abbes, Algeria

***Abstract*—Electrostatic separators are not commonly used for the selective sorting of different sorts of metals contained in a granular mixture. However, the separation might be possible if their characteristics (density, conductivity, size…) are different enough. The aim of this article is to evaluate the feasibility of sorting tinned and bare copper strands (length: 2 to 5 mm; diameter: 0.8 to 1.6 mm) contained in granular electric cable wastes, using a roll-type electrostatic separator with three different high-voltage electrode configurations: plate, S-shaped and reverse S-shaped. Experimental design methodology is used to investigate the effects of three factors: high-voltage applied to the electrode system, inclination of the high-voltage electrode, inter-electrode distance. The recovery and purity of the bare copper product are evaluated for each experiment. The best results of the electrostatic separation experiments are obtained with the reversed S-shaped electrode configuration (recovery of 55.4% of the bare copper wire, in a product having a copper content of 85.1%). Numerical modelling and experimental visualization of particle trajectories facilitate the interpretation of the electrostatic separation experimental results.**

## I. INTRODUCTION

Roll-type corona-electrostatic separators are mostly use for the selective sorting of conductive particles from non-conductive granular mixtures [1-8]. In these systems, an electric field is created between a grounded cylinder and one or more electrodes connected to a high-voltage supply. These separators process ores, wastes or agricultural matter.

When this type of electrostatic equipment is used to separate conductive and non-conductive materials from electric cable wastes, several metals can be recovered as one product. The recycling of such products is difficult or impossible [9, 10]. The various metals should be separated prior to their further processing.

Electrostatic separators are not commonly used to process different sorts of metals. However, some numerical studies have been made [11, 12] and show that, with special electrode configurations, separation might be possible.

The aim of this paper is to evaluate the capability of three electrode configurations to increase the copper content of a product containing bare and tinned copper electric wire wastes. Numerical computation and experimental visualization of the trajectories will help the interpretation of the separation results.

## II. MATERIALS AND METHOD

The granular mixture under study is a conductive product recovered after the electrostatic separation of a specific electric wire waste. The mixture is composed of $m_{bCu}$ = 45.8% bare copper and $m_{tCu}$ = 54.2% tinned copper wires. The length of the wire particles that compose this product (Fig. 1) ranges between 2 mm and 5 mm. The bare copper particles are characterized by a diameter range from 0.10 mm to 0.16 mm. The tinned copper particles diameter is 0.10 mm. The thickness of the tin layer is less than $t$ = 10 µm. So, the copper content in the initial mixture is roughly 82.6%, calculated with the formula:

$$Cu_{total} = m_{bCu} + k_{tCu} \times m_{tCu} \qquad (1)$$

where $k_{tCu}$ = 0.68 is the copper content of tinned copper, estimated for an average value of the tin layer thickness $t$ = 10 µm.

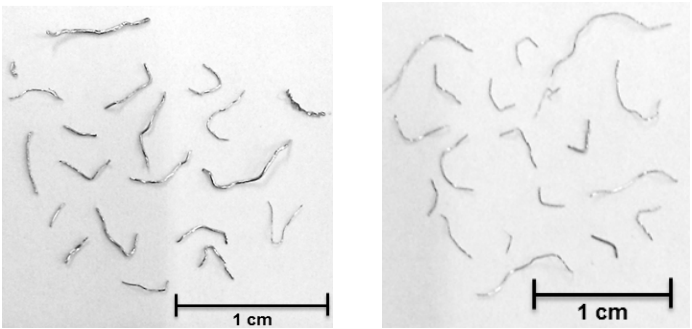


(a) (b)

Fig. 1. (a) Bare copper particles and (b) tinned copper particles from grinded electric cable wastes.

Experiments have been made on a roll-type electrostatic separator (CARPCO, Inc) with new electrode configurations (Fig. 2). In these separators, a vibratory electromagnetic feeder (1) brings the particulate mixture onto the surface of a rotary cylindrical grounded electrode (2). An electric field is created between the roll electrode and a static one (3), which are connected to a high voltage supply. Subjected to this electric field, the conductive particles acquire by electrostatic induction an electric charge the polarity of which is similar to that of the electrode they are in contact with. If the electric force exerted on them is strong enough, the particles are attracted by the static electrode, detach from the grounded electrode, and have different trajectories following their specific density, shape, volume… They are recovered in the collector (4) which is composed of 15 compartments.

Three electrode configurations were used. In configuration **#1** (Fig. 2) a perfectly flat electrode was connected to the high voltage supply. A S-shaped electrode was used in configurations **#2** and **#3**.

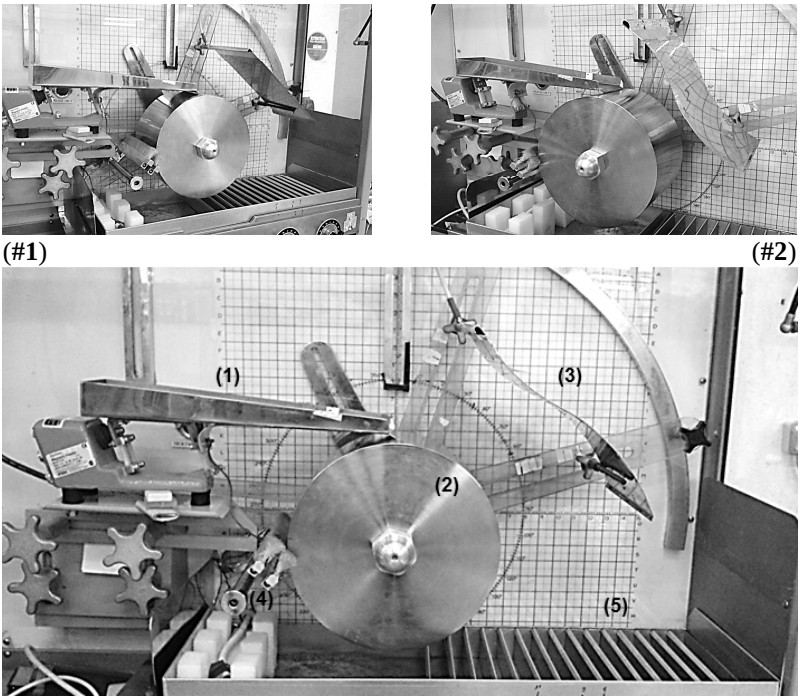


Fig. 2. Lab roll-type electrostatic separator (CARPCO, Inc.). (1) Electromagnetic feeder; (2) Rotating cylindrical electrode connected to the ground; (3) High-voltage plate electrode ((**#1**) Flat; (**#2**) Reversed-S-shaped; (**#3**) S-shaped); (4) Brushes; (5) 15-compartment collector.

In an electrostatic process, the conductive particles carried by the roll electrode are affected by three forces (Fig. 3): the electric (Coulomb) force $F_e$ due to the static electrode, the gravitational force $F_{gn}$ and the centrifugal force $F_c$ [13].

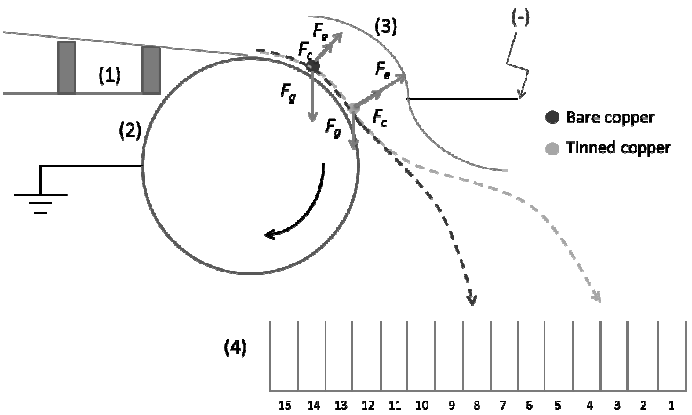


Fig. 3. Forces which act on particles in roll-type electrostatic separators (configuration **#2**)

The electric force is expressed by:

$$F_e = qE \quad (1)$$

where $q$ [C] is the charge acquired by electrostatic induction, and $E$ [V·m$^{-1}$] designates the local electric field. The charge of a cylindrical conductive particle of length $l$ [m] and radius $r$ [m] is:

$$q = 2\pi r l E \varepsilon_0 \quad (2)$$

where $\varepsilon_0$ is the permittivity of air, considered equal to that of free space:

$$\varepsilon_0 = \frac{1}{4\pi 9.10^9} \text{ [F·m}^{-1}\text{]} \quad (3)$$

The gravitational force is:

$$F_g = mg \quad (4)$$

where $m$ [kg] is the mass of the particle and $g$ the gravity constant (9.81 m.s$^{-2}$).

The formula used to express the centrifugal force is:

$$F_c = m\omega^2 R \quad (5)$$

with $\omega$ [rad.s$^{-1}$]: the angular speed of the roll electrode; $R$ [m]: the radius of roll electrode.

A first series of fractional factorial experimental designs [14, 15] was carried out, to roughly evaluate the effects of three factors (Fig. 4):

- Inclination angle of the static electrode connected to high-voltage ($\alpha$, [°]),
- High-voltage applied to the static electrode ($U$, [kV]),
- Distance between the roll surface and the high-voltage electrode ($d$, [mm]).

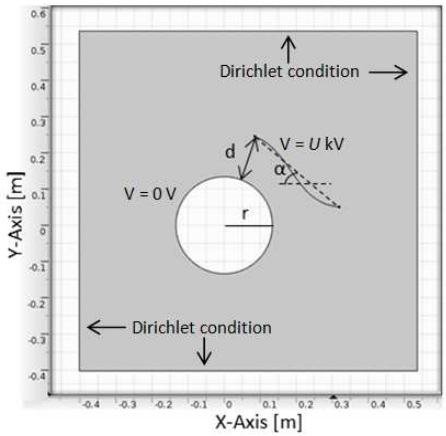


Fig. 4. Control variables and geometrical characteristics of electrode configuration **#2**.

Two process responses are considered in the present study:

- Recovery of bare copper (*REC bCu*, [%]),
- Recovery of tinned copper (*REC tCu*, [%]).

The particles recovered in each compartment were affected to one of the following products: “tinned copper product”, “middling product” or “bare copper product”. The tinned copper product corresponds to a mixture composed at least of 65% tinned copper. Middling product has approximatively the same composition than the initial mixture (45.8% bare copper and 54.2% tinned copper) and the bare copper product is at least composed of 50 % bare copper.

Preliminary tests were done to establish the variation range for each of the four factors (Table 1). Within these ranges, no electric arc appears and both bare copper and tinned copper are correctly separated.

In some cases, a fast camera (Photron APX RS; 1000 frames/s; shutter: 1/10,000 s; resolution: 1024 x 1024 pixels; duration of one experiment: 6.144 s) was used to visualize the particle trajectories and compare them to numerical simulations.

TABLE 1: FACTOR VARIATION RANGES

| Levels | α [°] | U [kV] | d [mm] |
|---|---|---|---|
| -1 | 30 | 15 | 100 |
| 0 | 40 | 20 | 125 |
| 1 | 50 | 25 | 150 |

## III. ELECTRIC FIELD COMPUTATION AND NUMERICAL MODELING OF PARTICLE TRAJECTORIES

The electric field strength in the active zone of each configuration was calculated with a commercial software (Fig. 5). The maximum electric field for the configuration **#1** is less than for the two others, which means that the separation is likely to be less efficient. For the configurations **#2** and **#3**, the maximum values of the electric field not are at the same place. This could change the results of the separation because the detachment angle will not be the same.

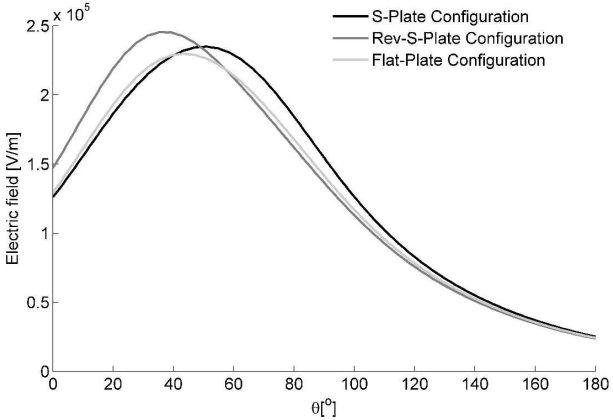


Fig. 5. Electric field distribution at the surface of the grounded electrode, for $\alpha$ = 40°, $U$ = 20 kV, $d$ = 125 mm.

The algorithm of particle trajectory computation was established under the following commonly-accepted assumptions [16-19]: (1) The particle is a perfect conducting cylinder with radius $r$ and a specific mass $\rho$; (2) The particle charges instantly through electrostatic induction, at the maximum value given by Félici's formula [20]; (3) The distance between two adjacent particles is sufficiently large so they do not affect each other; (4) The space is homogeneous, isotropic with the permittivity ε; (5) The electric force before the detachment is [20]: $F_e = 0.715qE$ , and after detachment: $F_e = qE$; and (6) The tribocharging effects are negligible. The program for the computation and plotting of conducting particle trajectory was written in MATLAB language, with a time step of 0.1 ms.

The first step in computation of particle trajectory is evaluation of the detachment angle (i.e angle on the surface of grounded roll at which the particle lifts-off). A particle can detach from the grounded electrode if the following condition is satisfied:

$$F_g \times \sin(\theta) = F_e + F_c \tag{6}$$

$$\sin(\theta) = \frac{F_e + F_c}{F_g} \tag{7}$$

where $F_g$ is the gravity force of particle; $F_e$ is the electric force; $F_c$ is the centrifugal force. When the particle detaches from rotating roll, the position of particle in the air is given by the following equations:

$$x_{i+1} = x_i + V_x(x_i, y_i)dt + 0.5a_x(x_i, y_i)dt^2 \tag{8}$$

$$y_{i+1} = y_i + V_y(x_i, y_i)dt + 0.5a_y(x_i, y_i)dt^2 \tag{9}$$

with:

$$V_x(x_i, y_i) = V_x(x_{i-1}, y_{i-1}) + a_x(x_{i+1}, y_{i+1})dt \tag{10}$$

$$V_y(x_i, y_i) = V_y(x_{i-1}, y_{i-1}) + a_y(x_{i+1}, y_{i+1})dt \tag{11}$$

$$a_x(x_i, y_i) = \frac{-6\pi\mu r V_x(x_{i-1}, y_{i-1}) + q_d E_x(x_{i-1}, y_{i-1})}{m} \tag{12}$$

$$a_y(x_i, y_i) = \frac{6\pi\mu r V_y(x_{i-1}, y_{i-1}) + q_d E_y(x_{i-1}, y_{i-1})}{m} - g \tag{13}$$

where: $V_x$ and $V_y$ are respectively the $x$-component and $y$-component of particle speed; $a_x$ and $a_y$ are respectively the $x$-component and $y$-component of particle acceleration; $\eta = 1.81 \times 10^{-5}$ is the air drag coefficient.

Numerical simulation of particle trajectories (Fig. 6) shows that the reverse-S-plate should give the best separation result, as for this configuration difference between tinned and bare copper particle trajectories is the more important.

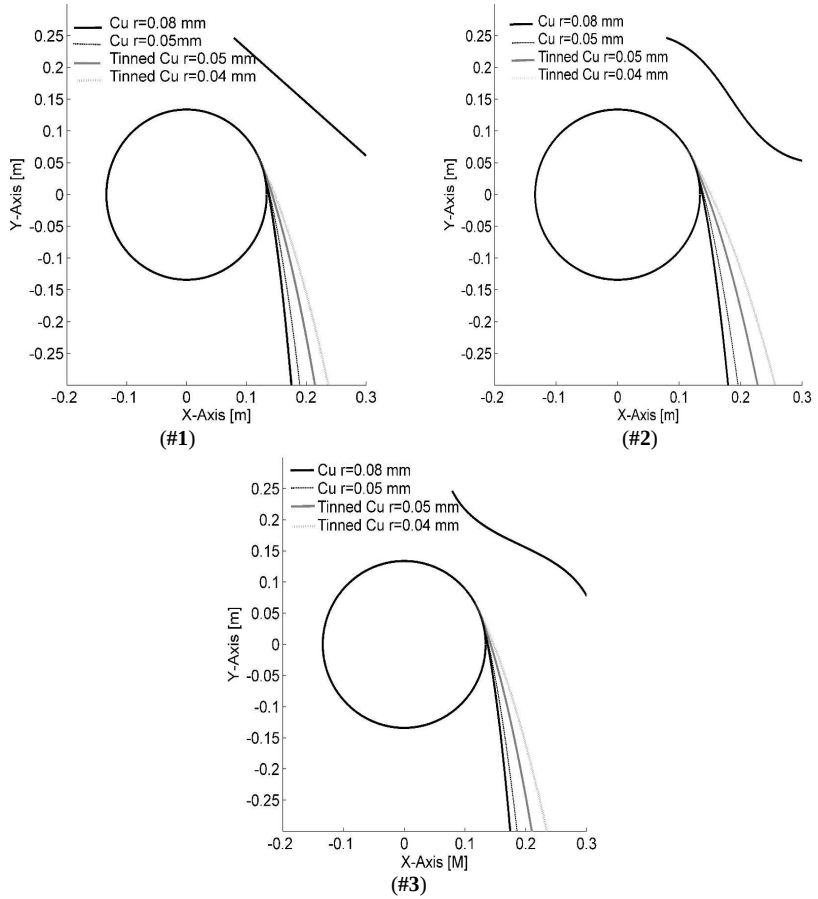


Fig. 6. Numerical simulation of particle trajectories for each configuration computed with MATLAB, for $\alpha$ = 40°, $U$ = 20 kV, $d$ = 125 mm.

## IV. RESULTS

During the first sets of 9 experiments carried out for each electrode configuration (three experiments for each high, zero and low level of each factor, at the zero level of the two others), the flow rate was adjusted at 4.5 $kg.h^{-1}$ and the mass of the sample to be separated was 50 g. The results of these experiments are given in Tables 2, 3 and 4. Clear grey cells are considered as tinned copper product and dark grey cells correspond to bare copper product. Shaded cells correspond to the middling product.

The repeatability is good in all cases, which means that the experimental errors are not important. Collecting boxes may contain different products, depending on factor values. For instance, the $8^{th}$ compartment in configuration **#1** contains tinned copper for (-1,0,0) factor levels, mixed product for (0,-1,0) and bare copper product for (1,0,0).

TABLE 2: RESULTS OF THE FRACTIONAL FACTORIAL EXPERIMENTAL DESIGN FOR CONFIGURATION **#1**

| Voltage Level | Angle Level | Distance Level | m1 | m2 | m3 | m4 | m5 | m6 | m7 | m8 | m9 | m10 | m11 | m12 | m13 | m14 | m15 | bCu Mass | tCu Mass |
|---|---|---|---|---|---|---|---|---|---|---|---|---|---|---|---|---|---|---|---|
| -1 | 0 | 0 | 0.015 | 0.017 | 0.053 | 0.091 | 0.202 | 0.345 | 0.709 | 1.53 | 4.558 | 37.396 | 3.147 | 0.855 | 0.417 | 0.25 | 0.186 | **42.251** | **2.962** |
| 1 | 0 | 0 | 3.351 | 2.119 | 1.979 | 2.108 | 2.524 | 3.379 | 4.708 | 5.888 | 12.665 | 5.907 | 1.728 | 1.096 | 0.786 | 0.527 | 0.407 | **35.371** | **9.557** |
| 0 | -1 | 0 | 0.313 | 0.313 | 0.418 | 0.601 | 0.885 | 1.37 | 2.231 | 3.463 | 8.853 | 25.779 | 2.699 | 1.097 | 0.664 | 0.319 | 0.288 | **38.428** | **6.131** |
| 0 | 1 | 0 | 1.665 | 1.262 | 1.462 | 0.873 | 2.473 | 3.249 | 4.49 | 6.22 | 13.877 | 8.47 | 1.87 | 1.07 | 0.686 | 0.434 | 0.34 | **35.997** | **5.262** |
| 0 | 0 | -1 | 1.738 | 1.148 | 1.246 | 1.629 | 2.035 | 2.694 | 3.726 | 5.491 | 12.041 | 12.643 | 2.172 | 1.04 | 0.728 | 0.477 | 0.372 | **33.387** | **7.796** |
| 0 | 0 | 1 | 0.315 | 0.391 | 0.504 | 0.712 | 1.054 | 1.612 | 2.653 | 4.247 | 10.21 | 22.587 | 2.687 | 1.143 | 0.633 | 0.355 | 0.268 | **37.883** | **7.241** |
| 0 | 0 | 0 | 0.816 | 0.588 | 0.77 | 1.045 | 1.369 | 1.983 | 3.173 | 4.851 | 12.658 | 16.299 | 2.7 | 1.394 | 0.76 | 0.475 | 0.357 | **34.286** | **6.571** |
| 0 | 0 | 0 | 0.75 | 0.569 | 0.696 | 0.968 | 1.335 | 2.054 | 3.314 | 4.655 | 11.765 | 17.533 | 2.809 | 1.276 | 0.746 | 0.394 | 0.322 | **34.523** | **6.372** |
| 0 | 0 | 0 | 0.65 | 0.539 | 0.695 | 0.887 | 1.26 | 1.844 | 3.128 | 4.669 | 10.602 | 19.299 | 2.801 | 1.334 | 0.742 | 0.418 | 0.33 | **35.196** | **5.875** |

TABLE 3: RESULTS OF THE FRACTIONAL FACTORIAL EXPERIMENTAL DESIGN FOR CONFIGURATION **#2**

| Voltage Level | Angle Level | Distance Level | m1 | m2 | m3 | m4 | m5 | m6 | m7 | m8 | m9 | m10 | m11 | m12 | m13 | m14 | m15 | bCu Mass | tCu Mass |
|---|---|---|---|---|---|---|---|---|---|---|---|---|---|---|---|---|---|---|---|
| -1 | 0 | 0 | 0.083 | 0.098 | 0.221 | 0.302 | 0.645 | 1.045 | 1.968 | 3.325 | 11.334 | 25.354 | 2.926 | 1.247 | 0.584 | 0.364 | 0.219 | **30.694** | **7.687** |
| 1 | 0 | 0 | 4.844 | 2.688 | 2.377 | 2.53 | 3.066 | 3.58 | 4.806 | 5.779 | 9.839 | 3.529 | 1.893 | 1.396 | 0.981 | 0.838 | 0.714 | **20.424** | **12.439** |
| 0 | -1 | 0 | 0.405 | 0.351 | 0.437 | 1.085 | 0.977 | 1.335 | 2.151 | 3.807 | 10.091 | 22.743 | 3.268 | 1.439 | 0.703 | 0.447 | 0.34 | **32.834** | **6.741** |
| 0 | 1 | 0 | 2.238 | 1.931 | 2.187 | 2.802 | 3.322 | 3.831 | 4.887 | 6.969 | 11.125 | 3.78 | 1.84 | 1.518 | 0.968 | 0.763 | 0.714 | **22.981** | **12.48** |
| 0 | 0 | -1 | 3.548 | 2.013 | 2.059 | 2.596 | 2.837 | 3.401 | 4.985 | 6.192 | 11.104 | 4.508 | 2.166 | 1.363 | 0.974 | 0.777 | 0.663 | **30.19** | **10.216** |
| 0 | 0 | 1 | 0.289 | 0.26 | 0.396 | 0.647 | 0.933 | 1.408 | 2.208 | 4.167 | 10.98 | 20.692 | 4.317 | 1.767 | 0.789 | 0.415 | 0.305 | **28.285** | **10.308** |
| 0 | 0 | 0 | 1.532 | 1.02 | 1.132 | 1.352 | 1.772 | 2.519 | 3.571 | 5.532 | 15.359 | 10.875 | 2.172 | 1.145 | 0.576 | 0.402 | 0.335 | **31.766** | **10.64** |
| 0 | 0 | 0 | 1.629 | 0.984 | 1.067 | 1.335 | 1.882 | 2.583 | 3.531 | 5.371 | 14.732 | 11.601 | 2.026 | 1.188 | 0.622 | 0.432 | 0.362 | **31.704** | **10.896** |
| 0 | 0 | 0 | 1.707 | 1.175 | 1.316 | 1.506 | 1.955 | 2.734 | 3.6 | 5.304 | 12.465 | 11.633 | 2.702 | 1.456 | 0.776 | 0.443 | 0.428 | **29.402** | **12.04** |

TABLE 4: RESULTS OF THE FRACTIONAL FACTORIAL EXPERIMENTAL DESIGN FOR CONFIGURATION **#3**

| Voltage Level | Angle Level | Distance Level | m1 | m2 | m3 | m4 | m5 | m6 | m7 | m8 | m9 | m10 | m11 | m12 | m13 | m14 | m15 | bCu Mass | tCu Mass |
|---|---|---|---|---|---|---|---|---|---|---|---|---|---|---|---|---|---|---|---|
| -1 | 0 | 0 | 0.007 | 0.033 | 0.075 | 0.153 | 0.261 | 0.438 | 0.793 | 0.1598 | 4.761 | 32.902 | 4.991 | 1.387 | 0.72 | 0.436 | 0.402 | **40.838** | **1.9198** |
| 1 | 0 | 0 | 3.209 | 2.059 | 2.077 | 2.303 | 2.944 | 3.731 | 4.378 | 5.473 | 11.56 | 6.38 | 1.929 | 0.994 | 0.68 | 0.468 | 0.406 | **22.417** | **12.592** |
| 0 | -1 | 0 | 0.289 | 0.29 | 0.407 | 0.566 | 0.854 | 1.351 | 2.083 | 3.695 | 12.845 | 21.462 | 2.751 | 1.212 | 0.839 | 0.449 | 0.294 | **39.852** | **5.84** |
| 0 | 1 | 0 | 1.065 | 0.99 | 1.222 | 1.656 | 2.205 | 2.853 | 4.217 | 6.906 | 17.932 | 6.1716 | 1.881 | 0.935 | 0.577 | 0.389 | 0.323 | **28.2086** | **7.138** |
| 0 | 0 | -1 | 2.017 | 1.249 | 1.391 | 1.846 | 2.587 | 3.277 | 4.255 | 6.278 | 13.486 | 8.263 | 2.071 | 1.076 | 0.663 | 0.424 | 0.398 | **32.659** | **9.09** |
| 0 | 0 | 1 | 0.075 | 0.105 | 0.187 | 0.299 | 0.489 | 0.749 | 1.272 | 2.365 | 6.382 | 30.811 | 3.802 | 1.242 | 0.662 | 0.368 | 0.318 | **37.203** | **5.541** |
| 0 | 0 | 0 | 0.455 | 0.4 | 0.522 | 0.746 | 1.121 | 1.623 | 2.382 | 3.817 | 10.191 | 21.153 | 3.442 | 1.217 | 0.831 | 0.54 | 0.394 | **27.577** | **11.066** |
| 0 | 0 | 0 | 0.466 | 0.4 | 0.452 | 0.622 | 0.945 | 1.331 | 2.116 | 3.299 | 7.754 | 25.546 | 3.819 | 1.193 | 0.633 | 0.409 | 0.306 | **31.906** | **9.631** |
| 0 | 0 | 0 | 0.425 | 0.377 | 0.464 | 0.605 | 0.94 | 1.304 | 1.98 | 3.158 | 8.656 | 24.733 | 3.626 | 1.181 | 0.725 | 0.453 | 0.4 | **31.118** | **9.253** |

These studies show that the configuration **#1**, with the flat electrode connected to the high voltage supply is not efficient to separate bare and tinned copper mixture. The mass of bare copper product proves that its purity is never good. In fact for 50 g of mixture, 22.9 g of bare copper should be present but the "bare copper product" was at least 33 g in each experiment. This means that at least 10.1 g of tinned copper is also present in the "bare copper product", even when assuming that the tinned copper is recovered as a pure product, which is not true. The computation of the electric field in this configuration proved that the electric field is not intense enough to attract tinned copper particles. Therefore, this configuration was not retained for the rest of this study.

For each configuration, a part of the tinned copper was recovered in boxes 11 to 15. This is due to the fact that the small particles collide with the S-shaped electrode and bounce in these compartments. This may also decrease bare copper product purity.

For the configurations **#2** and **#3**, the electric field is more intense and gives a better separation. According to results of the fractional factorial experimental designs, each configuration has optimum values of the factors for which the copper purity and recovery are the best. The best purity of the "bare copper product" corresponds to the situation when the recovery of the tinned copper is at its maximum (Fig. 7).

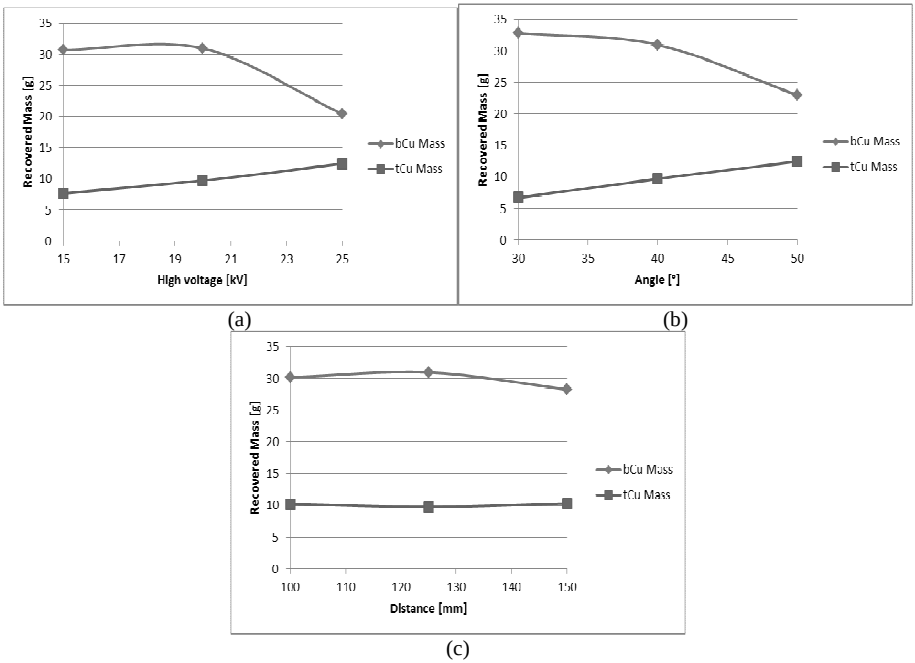


Fig. 7. Evolution of recovered bare and tinned copper according to (a) the high voltage value U; (b) the inclination angle α; (c) the distance between high-voltage and grounded electrode d; for configuration #2.

According to Fig. 7a, the quantity of bare copper product decreases with the increase of the high voltage value whereas the tinned copper product increases. The inclination angle has more influence on bare copper product than on tinned one (Fig. 7b). An increase of the distance from 125 mm to 150 mm is detrimental to the electrostatic separation (Fig. 7 c). The quantity of tinned copper product decrease and the bare copper one increase. That means that the electric field is not intense enough to attract tinned copper particles. So they are recovered with the bare copper product.

For configuration **#2**, the optimum values of the factors are:

- $\alpha = 50°$,
- $U = 25$ kV,
- $d = 150$ mm.

For the configuration **#3**:

- $\alpha = 40°$,
- $U = 25$ kV,
- $d = 125$ mm.

Two experiments were made for these optimal values of factors (table 5). When the reverse-S-plate was used (**#2**), box groups B1 and B4 (composed respectively of compartments 1 to 4 and 11 to 15) recovered the tinned copper product, B2 (compartments 5 and 6) contained the mixed product, and B3 (compartments 7 to 10) collected the bare copper product. For the S-plate (**#3**), five box groups were formed. The groups B1 (compartments 1 to 4) and B5 (compartments 11 to 15) contained the tinned copper product, whereas the group B3 that collected the copper product was composed only of compartments 8 and 9. The mixed product groups B2 and B4 respectively corresponded to compartments 5 to 7 and 10.

TABLE 5: SEPARATION RESULTS FOR OPTIMAL FACTORS VALUES FOR EACH ELECTRODE CONFIGURATION

| (#2) | | | | | | | | | | | | | | | | | |
|---|---|---|---|---|---|---|---|---|---|---|---|---|---|---|---|---|---|
| | | | B1 | | | | B2 | | B3 | | | | B4 | | | | |
| U [kV] | Angle [°] | d [mm] | m1 | m2 | m3 | m4 | m5 | m6 | m7 | m8 | m9 | m10 | m11 | m12 | m13 | m14 | m1 |
| 25 | 50 | 150 | 4.621 | 2.677 | 2.591 | 2.854 | 3.351 | 3.769 | 4.337 | 5.638 | 9.37 | 3.216 | 1.852 | 1.516 | 1.303 | 1.134 | 1.01 |
| Total [g] | | | 12.743 | | | | 7.120 | | 4.337 | 15.008 | | 3.216 | 6.819 | | | | |
| Copper content [%] | | | 79.62 | | | | 82.18 | | 84.29 | 85.60 | | 84.16 | 77.15 | | | | |
| (#3) | | | | | | | | | | | | | | | | | |
| | | | B1 | | | | B2 | | | B3 | | B4 | B5 | | | | |
| U [kV] | Angle [°] | d [mm] | m1 | m2 | m3 | m4 | m5 | m6 | m7 | m8 | m9 | m10 | m11 | m12 | m13 | m14 | m1 |
| 25 | 40 | 125 | 2.98 | 1.662 | 1.709 | 2.044 | 2.875 | 3.813 | 5.384 | 7.302 | 13.438 | 3.235 | 1.656 | 1.059 | 0.735 | 0.53 | 0.3 |
| Total [g] | | | 8.395 | | | | 12.072 | | | 20.74 | | 3.235 | 4.374 | | | | |
| Copper content [%] | | | 78.94 | | | | 81.63 | | | 85.44 | | 81.50 | 78.75 | | | | |

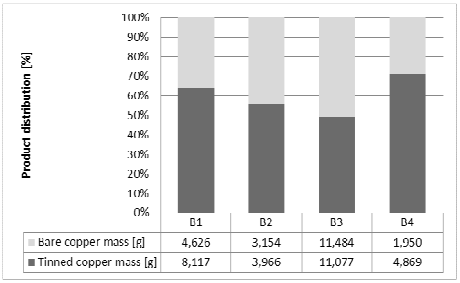


(**#2**)

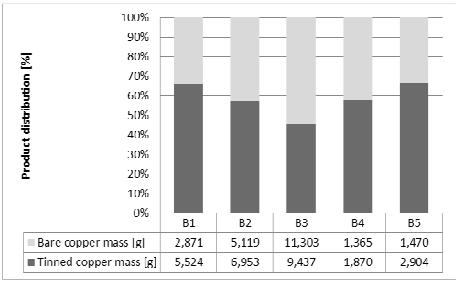


(**#3**)

Fig. 8. Distribution of bare and tinned copper products in each box group for each of the two configurations.

For these tests, the mass of bare and tinned copper on each box group was measured to compare the two configurations (Fig 8). Recovery and purity of the "bare copper product" were calculated as follows:

$$REC_{Cu} = \frac{m_{CuB3}}{m_{CuTot}} \times 100 \tag{6}$$

$$PU_{Cu} = \frac{m_{CuB3}}{m_{B3}} \times 100 \tag{7}$$

where $m_{Cu\ Bi}$ correspond to the mass of bare copper measured in the compartment *Bi*, $m_{CuTot}$ is the total mass of bare copper in all compartments and $m_{Bi}$ is the total mass of the compartment *Bi*.

For the configuration **#2** (reverse-S-plate electrode), 55.4% of the bare copper in the initial mixture is recovered in B3. With bare copper representing 53.6% of the mass of wire wastes collected in B3, the copper content of this product is 85.1%. With the S-plate electrode (configuration **#3**), the bare copper particles represent 54.5% of the mass in B3, but less bare copper (51%) was recovered than with the configuration **#2**. Also, tinned copper product recovery was poorer (31.6%) because a lot of product is mixed. In fact, for configuration **#3**, the mixed product represented 31.4 % of the total product, whereas it only was 14.5% for configuration **#2**. The configuration **#2** proved to be the best to separate bare and tinned copper product. The "bare copper product" obtained using the reverse-S-shape electrode configuration had a copper content of 85.1%, an increase of 2.5 % in comparison with the initial mixture.

## V. Discussion

More experiments were made to increase the copper content in the "bare copper product". The product collected in B3 was passed through the separator two times (Table 6) and it permits to recover 18.35% with an estimated copper content of 88.29 %. This value largely underestimates the actual copper contact of the obtained product, as the thickness of the tin layer is quite often less than half of the assumed value (10 µm).

TABLE 6: BARE COPPER PRODUCT RETREATMENT.

| First Pass | | | | | | | | | | | | | | | | | |
|---|---|---|---|---|---|---|---|---|---|---|---|---|---|---|---|---|---|
| | | | B1,1 | | | | B2,1 | | B3,1 | | | | B4,1 | | | | |
| U [kV] | Angle [°] | d [mm] | m1 | m2 | m3 | m4 | m5 | m6 | m7 | m8 | m9 | m10 | m11 | m12 | m13 | m14 | m15 |
| 25 | 50 | 150 | 9,24 | 5,35 | 5,18 | 5,71 | 6,7 | 7,54 | 8,674 | 11,28 | 18,7 | 6,432 | 3,7 | 3,03 | 2,61 | 2,27 | 2,03 |
| Total [g] | | | 12,743 | | | | 7,120 | | 4,337 | 15,008 | | 3,216 | 6,819 | | | | |
| Copper content [%] | | | 79,62 | | | | 82,18 | | 84,29 | 85,60 | | 84,16 | 77,15 | | | | |
| **Second Pass (B3,1)** | | | | | | | | | | | | | | | | | |
| | | | B1,2 | | | | B2,2 | | B3,2 | | | | B4,2 | | | | |
| U [kV] | Angle [°] | d [mm] | m1 | m2 | m3 | m4 | m5 | m6 | m7 | m8 | m9 | m10 | m11 | m12 | m13 | m14 | m15 |
| 25 | 50 | 150 | 2,67 | 1,64 | 1,72 | 2,12 | 2,32 | 2,86 | 3,674 | 4,825 | 8,39 | 2,911 | 1,6 | 1,15 | 0,82 | 0,71 | 0,67 |
| Total [g] | | | 8,150 | | | | 5,181 | | 3,674 | 13,21 | | 2,911 | 4,951 | | | | |
| Copper content [%] | | | 83,52 | | | | 85,47 | | 86,08 | 87,97 | | 86,56 | 81,73 | | | | |
| **Third Pass (B3,2)** | | | | | | | | | | | | | | | | | |
| | | | B1,3 | | | | B2,3 | | B3,3 | | | | B4,3 | | | | |
| U [kV] | Angle [°] | d [mm] | m1 | m2 | m3 | m4 | m5 | m6 | m7 | m8 | m9 | m10 | m11 | m12 | m13 | m14 | m15 |
| 25 | 50 | 150 | 0,85 | 0,57 | 0,62 | 0,88 | 1,18 | 1,49 | 2,164 | 3,059 | 6,13 | 1,281 | 0,46 | 0,28 | 0,2 | 0,17 | 0,18 |
| Total [g] | | | 2,921 | | | | 2,667 | | 2,164 | 9,185 | | 1,281 | 1,293 | | | | |
| Copper content [%] | | | 84,83 | | | | 86,41 | | 88,26 | 88,26 | | 88,53 | 82,97 | | | | |

This recovered quantity is not very important but it could be increased in an industrial facility. In fact, if three separating modules were placed in series, most of the boxes could be retreated. Fig. 9 shows a way to process this type of mixture which gives better results of copper recovery. As shown in Fig. 9, only the tinned copper product (B1.1 and B4.3) of the first separator is not treated again. About 70 % of all copper (B2.1 and B3.1) is treated again.

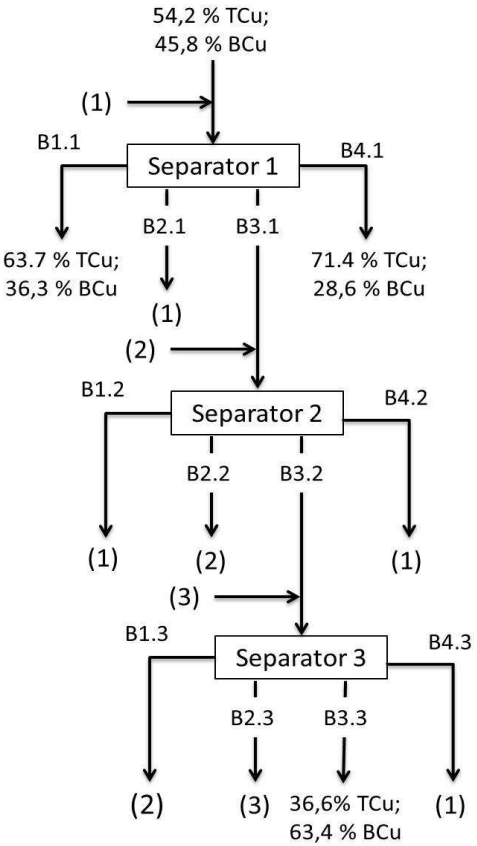


Fig. 9. Assumed product flow of a potential industrial facility.

Higher copper contents are difficult to obtain for the bare copper product. The physical characteristics of bare and tinned copper are quite similar. The specific density of bare copper is of 8960 kg/m$^3$ and an equivalent density of tinned copper wires is 8430 kg/m$^3$. Moreover, radius of tinned copper particles is inferior to the one of bare copper. This means that the ratio between the electrical and mechanical forces is higher in the case of tinned copper particles, which can detach easier than bare copper ones. Thus, a separation is possible.

The simulated trajectories of bare and tinned copper particles (Fig. 10) are different enough to expect a good separation of the two kinds of products. According to the numerical simulations, no particle collides with the reverse-S-shaped plate electrode, a prediction which is not confirmed by the experimental observations.

The measurements performed with the high-speed camera (Fig. 11) enable the evaluation of the predictive quality of these simulations and the explanation of the lower-than-expected purity of the separated products. Tinned copper trajectories 1 and 3, as well as all bare copper trajectories represented in Fig. 12 confirm that each type of particle has different trajectories and can be separated.

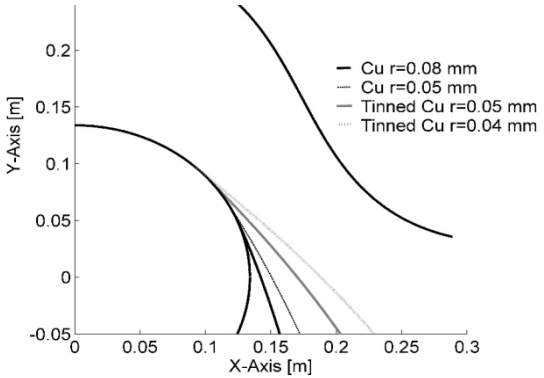


Fig. 10. Numerical computation of particle trajectories for configuration **#1**. $\alpha$ = 50°, $U$ = 25 kV, $d$ = 150 mm.

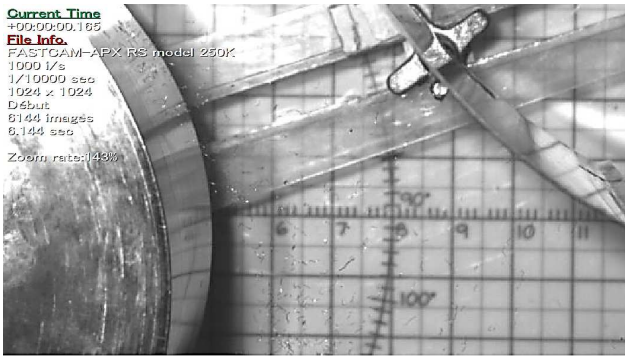


Fig. 11. High-speed-camera-displayed instant-image of tinned and bare copper particle positions in the roll-type separator (frame rate: 1,000 $s^{-1}$; shutter: 1/10,000 s; resolution: 1024x1024 pixels).

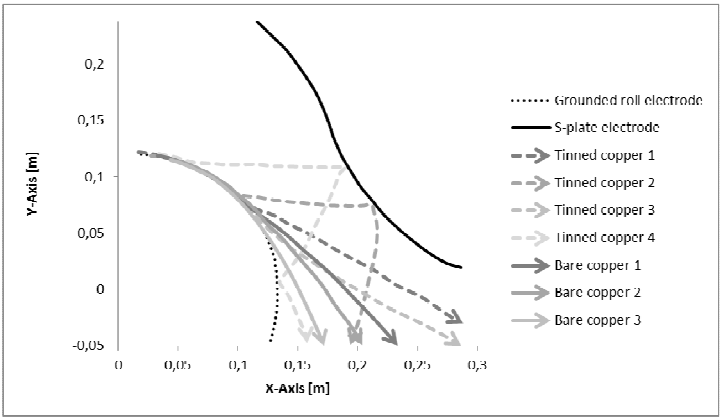


Fig. 12. High-speed-camera-visualization of tinned and bare copper particle trajectories, using the software Photron Fastcam Viewer (frame rate: 1,000 $s^{-1}$; shutter: 1/10,000 s; resolution: 1024x1024 pixels), for $\alpha$ = 50°, $U$ = 25 kV, $d$ = 150 mm.

But high-speed-camera results show also that some tinned copper particles (the smaller ones – trajectories 1 and 4 in Fig. 12) are attracted by the high-voltage reverse-S-plate electrode and collide with it. These particles could be recovered with the bare copper product or in compartments 11 to 15. This explains why bare copper purity is not as good as expected and why a lot of tinned copper particles are collected in the last compartments. This proves once more the necessity of experimental validation of numerical predictions.

## VI. Conclusions

The separation of tinned and bare copper particles is a difficult electrostatic separation because of the small differences between their characteristics. During this study, three geometries of high-voltage electrode were tested and lead to the following conclusions:

1) Utilization of an S-shaped plate gives the best results and permits to recover 55.4 % of bare copper in a product that contains more than 85% of copper

2) In spite of the fact that numerical modelling results predict a perfect separation of these two products, some tinned copper particles collide with the high-voltage electrode and bounce in wrong compartments, decreasing the purity of the bare copper product.

3) Good separation results are expected by using three separation modules in series, to reprocess the bare copper product, so that to attain the copper content required for its recycling.

3) Further work is needed to improve the numerical study to make it completely correspond to experimental results.

## References

[1] O. C. Ralston, "Electrostatic Separation of Mixed Granular Solids", Amsterdam, the Netherlands: Elsevier, 1961.

[2] J. E. Lawver and W. P. Dyrenforth, "*Electrostatic separation"*, A.D. Moore, U.S.A., 1973, pp 221–249.

[3] K. Haga, "Applications of the electrostatic separation technique", Marcel Dekker, U.S.A., *Handbook of electrostatic processes*, 1995, pp 365–368.

[4] L. Dascalescu, R. Morar, A. Iuga, A. Samuila, V. Neamtu, "Electrostatic separation of insulating and conductive particles from granular mixes," Particulate Science and Technology, vol. 16, 1998, pp. 25-42.

[5] Y. Higashiyama, and K. Asano, "Recent progress in electrostatic separation technology," Particulate Science and Technology, vol. 16, 1998, pp. 77–90.

[6] L. Dascalescu, A. Iuga, and R. Morar, "Electrostatic Technologies for the Recycling of non-ferrous metals and plastics from wastes" In *The Modern Problems of Electrostatics with Applications in Environmental Protection*, eds. I. I. Inculet, F. T. Tanasescu, and R. Cramariuc. Dordrecht: Kluwer Academic, 1999, pp. 77–87.

[7] R. Kohnlechner and L. Dascalescu, "New applications for "standard" electrostatic separators", Conf. Rec. IEEE IAS Annu. Meeting, Hong-Kong, 2005, pp. 2569–2572.

[8] K. Medles, L. Dascalescu, A. Tilmatine, A. Bendaoud and M. Younes, "Experimental modeling of the electrostatic separation of granular materials", Particulate Science and Technology, vol. 25, 2007, pp. 163–171.

[9] K. Popov, B. Grgur, and S.S. Djokic, Fundamental aspects of electrometallurgy, Berlin: Springer, 2002.

[10] Th. Zemb, C. Bauer, P. Bauduin, L. Belloni, C. Déjugnat, O. Diat, V. Dubois, J.-F. Dufrêche, S. Dourdain, M. Duvail, C. Larpent, F. Testard and S. Pellet-Rostaing, "Recycling metals by controlled transfer of ionic species: en route to ienaics", Colloid Polym. Sci., vol. 293, 2015, pp. 1-22

[11] M. Younes, A. Tilmatine, K. Medles, M. Rahli, and L. Dascalescu, “Numerical modeling of conductive particle trajectories in roll-type corona-electrostatic separators”, IEEE Trans. Ind. Appl., vol. 43, 2007, pp. 1130-1136.
[12] A. Younes, H. Sayah, M. Younes, A. Samuila and L. Dascalescu, “Behavior of conducting particles in a new electrostatic separator with two high-voltage electrodes”, Particulate Science and Technology, vol. 28, 2010, pp. 207–216.
[13] L. Dascalescu, A. Mizuno, R. Tobazéon and al., “Charges and forces on conductive particles in roll-type corona-electrostatic separators”, IEEE Trans. Ind. Appl., vol. 31, 1995, pp. 947–956.
[14] N.L. Frigon, and D. Mathews. *Practical Guide to Experimental Design*. New York: Wiley, 1996.
[15] L. Eriksson L., E. Johansson, N. Kettaneh-Wold, C. Wikstöm, and S. Wold. *Design of Experiments. Principles and Applications*. Umeaa, Sweden: Umetrics, 2000.
[16] J. Li, Z. Xu and Y. Zhou, “Theoretic model and computer simulation of separating mixture metal particles from waste printed circuit board by electrostatic separator”, J. of Hazardous Materials, vol. 153, 2008, pp. 1308–1313.
[17] J. Li, H. Lu, Z. Xu and Y. Zhou, “A model for computing the trajectories of the conducting particles form waste printed circuit board in corona electrostatic separators”, J. of Hazardous Materials, vol. 151, 2008, pp. 52–57.
[18] H. Lu, J. Li, J. Guo and Z. Xu, “Movement behavior in electrostatic separation: Recycling of metal materials form waste printed circuit board”, J. of Materials Processing Technology, vol. 197, 2008, pp. 101–108.
[19] J. Wu, J. Li and Z. Xu, “An improved model for computing trajectories of conductive particles in roll-type electrostatic separator for recycling metals form WEEE”, J. of Hazardous Materials, vol. 167, 2009, pp. 489–493.
[20] N. J. Félici, “Forces et charges de petits objets en contact avec une électrode affectée d’un champ électrique”, Rev. Gén. Elect., vol. 75, 1966, pp. 1145–1160.